Development of a Novel Lumbar Spinal Phantom for Rivanna Medical

By

Jacob Matriccino, Undergraduate Department of Biomedical Engineering
Victoria Parodi, Undergraduate Department of Biomedical Engineering
Adam Dixon, PhD, Rivanna Medical, Charlottesville, Virginia
Rachel Newman, Rivanna Medical, Charlottesville, Virginia

Word Count: 4638
Number of Figures: 6
Number of Tables: 2
Number of Equations: 0
Number of Supplements: 7
Number of References: 13

Approved: _____ Date: 4/29/2020

Adam Dixon, PhD, Rivanna Medical

Development of a Novel Lumbar Spinal Phantom for Rivanna Medical

Jacob Matriccino[a,1], Victoria Parodi[a,2], Adam Dixon, PhD[b], Rachel Newman[b]

[a] Biomedical Engineering Undergraduate at the University of Virginia
[b] Rivanna Medical, Charlottesville, Virginia
[1] jjm2dw@virginia.edu
[2] vmp3dr@virginia.edu

Abstract

Rivanna Medical manufactures Accuro, a handheld ultrasound device used to guide physicians during spinal anesthesia injections. Rivanna currently uses a commercial spinal phantom to allow doctors to practice the injection procedure with Accuro before using it on patients. A phantom is a device that mimics human tissue for the purposes of imaging and clinical training. Current phantoms have limitations such as lack of self-healing properties, limited longevity, opaque color, and high cost. The aim of this project was to design a novel lumbar spinal phantom that addresses three areas of focus: longevity, acoustic properties, and material properties. A novel phantom was created consisting of a skin layer, which mimicked human skin, and a tissue layer, which mimicked human tissue. The layer formulas were created by optimizing the ratios of 2-part polyurethane, terphenyl, and an ultrasound scatter to reduce the tackiness of the skin layer and increase the self-healing of the tissue layer. Due to its polyurethane construction, the phantom has a projected lifetime of more than 10 years. The developed phantom also demonstrated self-healing within 24 hours, further improving its lifespan. For acoustic properties, the phantom achieved a speed of sound statistically equivalent to that of human tissue at the 99.9% confidence interval ($p=0.00043$, $p=0.00023$). The phantom also shows attenuation similar to current phantoms and negligible insertion loss within medical ultrasound frequencies. The phantom has a transparent color, allowing doctors to view the injection point on the spine directly during training. Additionally, the skin layer had minimal tack, which makes for an easier and more realistic training experience. The novel phantom provides Rivanna Medical with an in-house product to complement their ultrasound device, support their business model by increasing company visibility and decreasing cost, and improve the longevity of spinal phantoms utilized by clinicians, ultimately delivering superior training performance.

Keywords: phantom, spinal, ultrasound, Rivanna Medical, epidural

Introduction

With the increase in medical devices, practitioners are constantly faced with the challenge of learning new procedures and technology. In the case of spinal anesthesia injections, imaging guidance methods such as X-rays or CT scans are used to guide physicians. However, the radiation associated with these imaging modalities prohibits their use for procedures on pregnant women.[1] Thus, physicians use manual palpation of the spine in order to identify a proper injection point. However, this procedure demonstrates inconsistent results. Currently, obstetric neuraxial analgesia shows a 12% failure rate with an overall catheter replacement rate of 7.1%, with 1.9% experiencing multiple replacements.[2] Since epidurals are primarily given during active labor, the time at which the patient is experiencing regular and intense contradictions, any time spent relocating the catheter equates to more patient pain.

As an alternative to this unreliable procedure, Rivanna Medical manufactures Accuro, a handheld ultrasound device. Accuro uses guidance algorithms which identify underlying anatomy and generate guidance imagery on a screen. These images are then used to locate a proper injection point. When compared to palpation, use of Accuro reduced spinal placement time from 6.5 minutes to 5 minutes.[3] Additionally, the incidence of the back

pain and spinal headache complications each decreased by 50% when using the device. The easy-to-use device improves the localization of the desired intervertebral space for first-attempt success. In turn, Accuro improves the efficiency of spinal anesthesia, the quality of medical care, and the confidence and comfort instilled in patients.

The adjustment from manual search to technology-assisted search requires a training device to allow doctors to practice with Accuro before using it on patients. Due to the location and the nature of the procedure, the training device needs to be a lumbar spinal phantom. A phantom is an artificial device that mimics human tissue for the purposes of imaging and clinical training.[4] This capstone project will work with Rivanna Medical to develop an in-house lumbar spinal phantom to allow doctors to train with Accuro.

To administer this procedure with Accuro, doctors are currently trained with the help of a commercial spinal phantom. This phantom is displayed in Supplemental Figure 1. However, this spinal phantom and other contemporary commercial phantoms have issues which limit their usage with Rivanna's Accuro device. First, phantoms available today do not self-heal.[5] Self-healing is defined as a material's ability to automatically form new bonds when old bonds are broken due to some injury of the material, without human intervention.[6] The lack of self-healing in current phantoms can cause unfavorable outcomes. First, the phantom accumulates needle tracks as multiple clinicians practice the procedure on the device. Needle tracks are channels left in the phantom's material when a needle punctures it. This is a problem because accumulating needle tracks could interfere with Accuro's spinal identification algorithms. The malfunctioning algorithms could discourage clinicians from using Accuro as they may perceive it to be ineffective. The accumulation of needle tracks also limits the longevity of the phantom, as it will have to be replaced when the tracks consistently interfere with device training.

Another limitation of Rivanna's current spinal phantom and many other commercially available phantoms is that they are constructed from hydrogels.[5,7] The bond structure of a hydrogel contains water, meaning that the phantom is prone to dry out over time, a process called desiccation.[5] This is especially the case if the phantom membrane is broken, exposing the hydrogel to air.[8] Desiccation limits phantom longevity, increasing replacement costs for doctors and hospitals to implement the Accuro device. The current spinal phantom has to be replaced each year due to hydrogel desiccation.[5] If the phantom is not made of a hydrogel, it is constructed from polyurethane. This material is more durable, having a projected lifespan of at least 10 years.[8,9] However, current polyurethane phantoms have a speed of sound near 1450 m/s, 90 m/s lower than that of human tissue.[9] This causes distance distortion, as ultrasound devices assume a speed of sound of 1540 m/s.

A novel lumbar spinal phantom will be developed to train doctors in the use of Accuro. The new spinal phantom functions specifically as a complement to Rivanna's ultrasound device, which has requirements for phantom depth and acoustic attenuation. The in-house lumbar spinal phantom decreases costs for Rivanna by providing a phantom at 1/4th the cost of the current commercial phantom. The phantom also decreases costs for clinicians, as it needs replacement less often. This is due to the unique formulation of self-healing polyurethane. The polyurethane makes the phantom immune to desiccation, while the self-healing properties repair needle track damage. Finally, the phantom allows clinicians to see through the translucent "tissue" and "skin" layers and observe the injection point in the 3D printed spine. The development of a novel lumbar spinal phantom improves Rivanna's business model by introducing a more affordable phantom and increasing company visibility by offering a novel, innovative, self-healing phantom.

The spinal phantom capstone project will complete the formulation, testing, and commercialization of a lumbar spinal phantom. This phantom provides Rivanna Medical with an in-house product to complement their ultrasound device and support their business model by increasing company visibility and decreasing cost. Additionally, the new design improves the longevity of spinal phantom utilized by clinicians, ultimately delivering superior performance when training to administer spinal anesthesia.

Results

Skin and Tissue Layer Chemical Formulation and Layer Combination

To develop the chemical formulation of the skin and tissue layer, a two-part polyurethane (RM16 A/B), a filler (terphenyl), and an ultrasound scatterer were used. The finalization of the layers was based on iterative testing of the mass ratio of RM16A to RM16B to terphenyl based on Table 1. The mass ratio of the tissue layer was determined to be 10 lbs of RM16A: 8 lbs of RM16B to 2 lbs of terphenyl. The mass ratio of the skin layer was determined to be 10 lbs of RM16A to 9.5 lbs of RM16B to 2 lbs of terphenyl. Both layers exhibited translucence in their final formulation.

Table 1: This table displays the phantom layer requirements. *Iterative ratio testing was performed for the formulation of the 3-D printed spine located within a polyurethane tissue layer with a stiffer polyurethane layer on top replicating the skin layer.*

	Tackiness	Self-Healing
Skin Layer	Low tack	Desirable, but unnecessary
Tissue Layer	Any tack acceptable	Necessary

Quality testing on the developed polyurethane tissue layer and stiffer polyurethane skin layer examined tackiness and self-healing properties. The quality testing verified that each layer matched its desired traits according to Table 1. The tissue layer's level of tack does not matter since it will not be in direct contact with physicians. This is because the layer will be covered by the skin layer. However, the tissue layer requires self-healing properties because it will sustain the most damage from each needle injection. Also, since the tissue layer makes up the majority of the phantom, any sustained damage will have a greater effect on ultrasound readings. Practicing physicians will be injecting the phantom with the practice needle regularly, so the tissue layer requires self-healing properties. If the tissue layer did not self-heal, this would be detrimental to the physician experience because of needle track accumulation. If needle tracks accumulate to a degree where they are picked up by the Accuro device, the anatomical identification algorithm could malfunction, leading to poor device performance. The skin layer requires a low tack because the physicians practicing with the phantom will have direct contact with it. Having the skin layer be excessively tacky would not create a realistic simulation of the procedure and would make the layer more prone to damage. However, self-healing properties are less important for the skin layer, because of its small volume compared to the tissue layer. The skin layer barely registers on the ultrasound, so any damage it sustains is negligible in terms of Accuro's identification algorithms.

Upon finalization of chemical formulations, the skin and tissue layer were combined. This was done to test the two formulation's ability to adhere to each other. The layers successfully adhered to each other and created a consistent boundary that is not visible on the ultrasound. The combined skin-tissue layer continued to exhibit translucence, with the boundary between the layers only visible from the side. This boundary visibility was eliminated in the final phantom design.

Self-Healing Testing

To observe the tissue layer's self-healing ability, testing was performed. First, the tissue layer of the spinal phantom was "injured" to leave a needle track in the spinal phantom as displayed in Supplemental Figure 2. Then, a time-lapse camera was used to record the self-healing progression of the spinal phantom. These images were analyzed to identify self-healing properties and timeframes. As recorded by the time-lapse video, the needle tracks decreased in size during the time period. The decrease in size of the needle tracks is displayed in Supplementary Figure 2. The majority of the needle tracks had disappeared by hour 7, with the tracks being almost completely invisible by hour 16.

Acoustic Characterization

Rivanna's tissue layer performance was evaluated and data was generated with respect to speed of sound, attenuation, surface tack, color, and phantom life. This information is summarized in Table 2. Additionally, the table compared these properties with human tissue and ATS, a commercially available polyurethane tissue mimic. Overall, the developed tissue layer has a speed of sound closer to human tissue than the ATS tissue mimic. To confirm the statistical equivalence of the speed of sound of Rivanna's tissue layer to that of

Table 2: This table summarizes the performance of the RIVANNA tissue layer with respect to speed of sound, attenuation, surface tack, color, and phantom lifetime. *The column labelled ATS represents a commercially available polyurethane tissue mimic sold by ATS. Overall, the RIVANNA tissue layer has a speed of sound that is closer to that of human tissue than the ATS tissue mimic. It should be noted that surface tack, color, and phantom lifetime apply only to Rivanna-tissue layer and ATS, not human tissue. One other major difference is that the color of the ATS tissue mimic is amber. Meanwhile, the RIVANNA tissue layer as well as the skin layer are transparent, which meets a predetermined phantom creation goal for the project. Additionally, although the surface tack is lower for the ATS phantom, the RIVANNA tissue layer would normally be covered with a skin layer, reducing surface tack to "minimal." This minimal surface tack is acceptable and fulfills a goal for phantom creation.*

Spec	RIVANNA - Tissue Layer	ATS	Human Tissue
SOS (m/s)	1526	1450	1540
Attn @ 3.5 MHz (dB/MHz-cm)	0.49	0.5	0.5 - 0.7
Surface Tack	Significant	None	N/A
Color	Transparent, Light Straw	Opaque, Amber	N/A
Phantom Lifetime	>10 yr	>10 yr	N/A

in vivo human tissue, a 2-tailed, 1-sample equivalence t-test was performed.[10] The t-test was performed with a 99.9% confidence interval. The alternative hypothesis was that the novel tissue layer would have a speed of sound that is within the equivalence interval of in vivo human tissue. The null hypothesis was that the speed of sound in Rivanna's tissue layer lies outside of the equivalence interval. The equivalence interval represents ±5% of the speed of sound in human tissue, 1540 m/s.[11] This meant that the confidence interval of the difference between the mean speed of sound of Rivanna's tissue layer (n=3) and the known speed of sound through human tissue had to be between 77 m/s and -77 m/s for the test to show significant equivalence. The t-test resulted in a Confidence Interval of (-55.00, 29.99). The p-value for the difference between the tested mean and the known speed of sound being less than or equal to -77 m/s was p = 0.00043, while the p-value for the difference being greater than or equal to 77 m/s was p = 0.00023. Since both p-values are below 0.001, the null hypothesis was rejected, the alternative hypothesis was accepted, and statistically significant equivalence was claimed. The report of this statistical test is available in Supplement Figure 3.

When comparing the developed tissue layer's surface tack, color, and lifetime with that of ATS, there are several differences. A summary of these differences can be found in Table 2. The color of the ATS tissue mimic is amber whereas the Rivanna tissue layer is transparent. The transparent tissue layer meets a predetermined phantom creation goal for the project. This is discussed further in the Discussion section. Additionally, although the surface tack is lower for the ATS tissue mimic, the Rivanna tissue layer would normally be covered with a skin layer, reducing the surface tack to "minimal."

Attenuation was measured to describe the rate at which energy is dissipated as a sound wave travels a certain distance through the materials. Attenuation was measured in four different mixtures by Acertara. Mixture A had a 1:1 A:B polyurethane ratio, Mixture B was the skin layer, Mixture C was the tissue layer, and Mixture D had a 5:6 A:B polyurethane ratio. As seen in Figure 1, attenuation over a range of ultrasound signal frequencies was measured in the four different mixtures. Each material showed similar attenuation in the frequency range of medical ultrasounds, which is normally 1-10 MHz.[5] Table 2 shows that ATS and the Rivanna phantom have a very similar attenuation at 3.5 MHz.

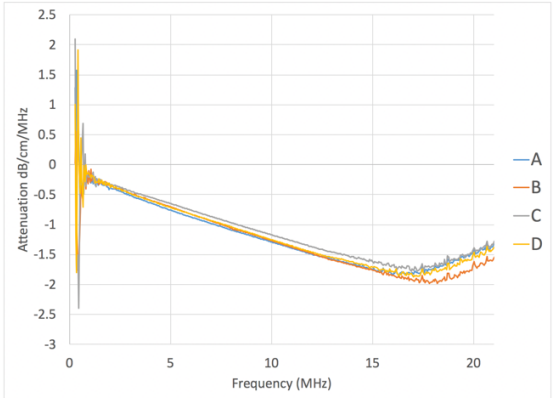

Figure 1: This figure shows attenuation (dB/cm/MHz) paired with the frequency of the ultrasound signal in the four different mixtures under study. *Mixture A had a 1:1 A:B polyurethane ratio, Mixture B was the skin layer, Mixture C was the tissue layer, and Mixture D was a 5:6 A:B polyurethane ratio. Each material shows similar attenuation in the frequency range of medical ultrasound, which is normally 1 - 10 MHz.*[5]

Insertion loss was measured to describe how much acoustic energy fails to enter the material when

ultrasound is applied to its surface. A highly negative insertion loss value means that much of the initial acoustic energy never entered the material. Figure 2 shows the insertion loss/cm over a range of frequencies of ultrasound signal in the same four mixtures as stated above. Each material showed similar insertion loss in the frequency range of medical ultrasound, 1-10MHz. Unfortunately, these data cannot be compared to the insertion loss exhibited by the ATS phantom, as this data is proprietary.

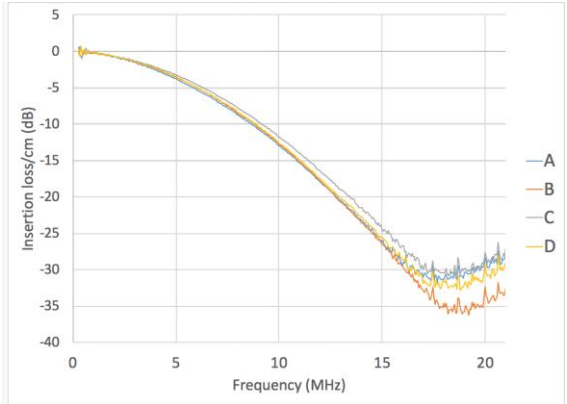

Figure 2: This figure shows insertion loss/centimeter paired with the frequency of the ultrasound signal in the four different mixtures under study. *Mixture A had a 1:1 A:B polyurethane ratio, Mixture B was the skin layer, Mixture C was the tissue layer, and Mixture D was a 5:6 A:B polyurethane ratio. Each material shows similar insertion loss in the frequency range of medical ultrasound, which is normally 1 - 10 MHz.*[5]

Curing Method Finalization

To ensure quality ultrasound testing, phantom viability, and minimize settling of scatterers, the curing method was finalized. This was completed by manipulating the curing time period as well as the amount of heat exposure during the curing process. In order to finalize the curing method, ultrasound scatterer settling testing was performed to indicate which curing procedure produced minimal scatter settling. Scatterer distribution is critical, as scatterers scatter the ultrasound signal, which replicates a process that occurs naturally in human tissue. Areas with fewer scatters show up darker on the ultrasound. These dark spots, if not appropriately located, could interfere with Accuro's identification algorithms because heterogeneous ultrasound scattering is not an expected behavior of human tissue.

Figure 3 shows the results of these tests. Figure 3A shows scatter settling because it contains a dark area in the top-middle of the image. This dark area contains fewer scatterers than other areas, meaning

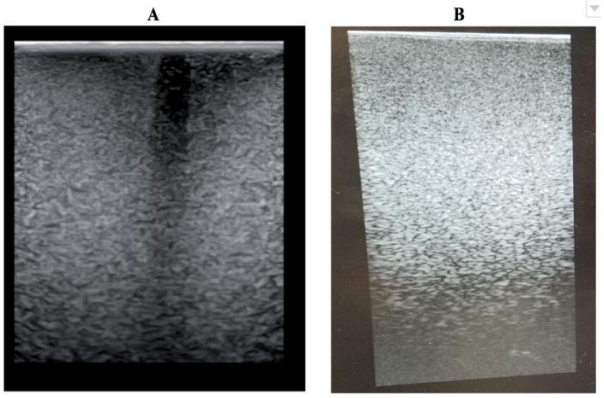

Figure 3: This figure shows the results of an ultrasound scatterer settling test, with Figure 3A showing scatterer settling and Figure 3B showing no scatterer settling. *These tests were conducted to examine which curing procedure to use to prevent the scatterers from settling. Based on these tests, it was determined that the curing procedure from Figure 3B should be used since this promoted homogeneous distribution of scatterers. The cure that produced Figure 3A was too slow and allowed the scatterer to settle. Scatterer distribution is important because scatterers, micron-dimensioned solid particles, scatter the ultrasound signal. This happens naturally in human tissue. Areas with fewer scatterers will show up dark on the ultrasound, as seen in the middle-top of Figure 3A. This could potentially interfere with the Accuro's identification algorithms because heterogeneous scatterer distribution does not mimic in vivo human tissue.*

that there is not a homogeneous scatterer distribution. The cure that produced Figure 3A was too slow and allowed the scatterers to settle. The phantom cures from the outside in, so scatterer settling in the middle of the test phantom means the cure was too slow. To demonstrate this concept numerically, the average pixel intensity and standard deviation of pixel intensity were measured for two areas in Figure 3A. This measurement was conducted in ImageJ. One area was on the left of the image where scatterer distribution was homogenous. The other area was the top-middle of the image where scatterers distribution was heterogeneous. The results are shown in Supplemental Table 1. The area with homogeneous scatterer distribution had a higher average pixel intensity of 114.87 than the heterogeneous area, which had an average intensity of 59.66. This meant that the area was nearly twice as bright and more accurately mimicked *in vivo* human tissue, which shows up bright under ultrasound. The area with homogeneous scatterer distribution also had a lower standard deviation of pixel intensity. The

homogeneous area had a standard deviation of 20.29 compared to 32.32 for the heterogeneous areas. A lower standard deviation means that there was less variation in pixel intensity, demonstrating a more homogeneous distribution of scatterers. The heterogeneous area, on the other hand had a pixel intensity standard deviation of more than 50% higher, meaning that there was more heterogeneity of scattering, which does not replicate human tissue. These findings were confirmed by the calculation of the coefficient of variation or the ratio of the standard deviation to the mean. The homogenous scatterer distribution had a much lower coefficient of variation of 0.177, indicating a more precise estimate, whereas, the heterogenous scatterer distribution had a much higher coefficient of variation of 0.542, demonstrating a greater level of dispersion around the mean.

Overall, Figure 3B shows a homogenous scatterer distribution, with roughly equal brightness throughout the area of concern. The darker area on the bottom of the image is not part of the test and was likely an artifact of the surface on which the test took place. Based on these tests, it was determined that the curing procedure from Figure 3B should be used since this promoted homogeneous distribution of scatters. This curing method is detailed below in the Materials and Methods section.

Discussion

The novel lumbar spinal phantom described in this paper effectively provides Rivanna Medical with an in-house product that will support their business-process model and allow doctors to practice with Rivanna's Accuro. As discussed in this paper, the project completed the chemical formulation, testing, and commercialization of the novel spinal phantom. The project created a new phantom by optimizing ratios of the 2-part polyurethane, terphenyl, and a scatterer to reduce tackiness for the skin layer and increase self-healing for the tissue layer.

Rivanna's design requirements were met in the development of the novel spinal phantom. The design requirements gave goals for phantom color, tack, and self-healing, as well as acoustic properties such as attenuation, insertion loss, and speed of sound. For phantom color, the design requirements necessitated a translucent phantom. As shown in Table 2, the tissue layer is translucent. The skin layer also obtained this property. A translucent color is unique among currently available spinal phantoms. This translucence will allow physicians to see through the material and observe the injection point in the spine directly as they conduct the injection. This is important because the visual aspect of the hand-eye coordination equation has been chronically overlooked in physician training.[12] Current spinal phantoms lack some of the visual cues used to control fine motor procedures, such as injections. This makes these training devices not as effective as they could be. The translucence of the Rivanna phantom ensures the connection of visual and manual cues.

For phantom tack, the skin layer was optimized for minimal tack according to the design requirements. This was done for three reasons. First, for practical reasons, a skin layer with a high tack would be less viable. This is because it is more likely to be stretched during the practice procedure. This stretching could result in tearing if the needle, Accuro, or other equipment are removed too suddenly. Secondly, physicians are likely to complain about a high tack skin layer being too sticky during the procedure.[5] This stickiness makes the phantom more difficult to practice with. Finally, a high tack skin layer does not replicate *in vivo* conditions, in which human skin has zero tack. A low tack skin layer creates a more realistic training process.

For phantom self-healing, the design requirements dictated that the phantom had to have self-healing abilities. As demonstrated in Supplemental Figure 2, the phantom has the ability to heal injuries within 24 hours. The injuries demonstrated in this figure were caused by a larger needle that would not be used for training. The training needle would have approximately 1/4th the diameter of the exaggerated needle. Thus, the self-healing demonstrated would likely be even quicker in a real training scenario. This is the result of optimizing the tissue layer for self-healing properties. The self-healing properties are unique among current phantoms. The self-healing will bolster an already long phantom lifespan by decreasing the effect of training on the integrity of the phantom. During layer formulation testing, it was observed that

tackiness and self-healing ability are directly correlated. The tissue layer's high tack corresponded with better self-healing outcomes, while the skin layer's low tack contributed to a lack of self-healing. This is likely due to a high tack material's elasticity. This elasticity likely complemented the inherent self-healing properties of the proprietary polyurethane mixture to more quickly close injuries to the phantom.

The design requirements for the acoustic properties were determined primarily by Rivanna's previous experience and knowledge with phantoms. According to Adam Dixon, the Rivanna correspondent, an attenuation similar to the ATS tissue mimic is an acceptable outcome for phantom development. Since the tissue layer has a very similar attenuation to that of the ATS tissue mimic at 3.5 MHz, the observed attenuation met the design requirement. Unfortunately, the attenuation at other frequencies cannot be compared because the full ATS attenuation data is proprietary. Having an attenuation similar to that of the ATS tissue mimic is important because it validates that despite the new properties attained by the development phantom, it still has similar baseline acoustic properties to the current market phantoms.

With respect to insertion loss, the requirements are flexible and determined by functional testing. Dixon states, "...we care about operations between 1-10 MHz, for which the insertion loss is negligible(very close to 0db)."[5] Thus, according to Rivanna, the spinal phantom's insertion loss is negligible in the frequency range of concern. This meets Rivanna's design requirement. Insertion loss being negligible is important for the same reason similar attenuation to the ATS tissue mimic is important. It validates that despite the new properties of the phantom, insertion loss will not have a significant impact on the ultrasound signal.

Regarding speed of sound, the design requirements gave a range of ±5% of the human tissue speed of sound in which the phantom's speed of sound would be acceptable. Statistically significant equivalence was claimed between the speed of sound of Rivanna's tissue layer and that of *in vivo* human tissue at the 99.9% confidence interval. Therefore, the developed spinal phantom met Rivanna's design requirements. This is important because the ultrasound device expects the speed of sound to be 1540 m/s, so any deviation will result in distortion of the ultrasound readout. Having the phantom's speed of sound be within the acceptability range limits the impact of this distortion.

Limitations existed for the capstone project. The required materials for the chemical formulation have expiration dates that may have limited the amount of reactivity of the skin and tissue layers. Human error, such as inconsistent mixing and imprecise measurement may have also posed an issue and delayed the finalization of the chemical formulation. Another possible reason for the delay of the chemical formulation timeline could have been the time period for the delivery of new materials. Additionally, there were limitations for the productization of the spinal canal. There were delays with the backfilling of the spine due to inhibitors that prevented the curing process. Similar to the limitation for chemical formulation, human error, such as inconsistent mixing and imprecise measuring may have created additional risks or delays. The project faced several limitations as a result of COVID-19. The group was no longer able to report to work in Rivanna's office. Therefore, the project had to be continued remotely. This meant that the capstone project was completed with three full-scale phantoms instead of five as originally projected.

Despite limitations, the project was able to capture the entire spinal phantom synthesis process and allow for future reproduction by Rivanna. It is assumed that there is reproducibility of the procedure based on the production of three full-scale phantoms. Based on this reproducibility assumption, next steps include the continuation of the commercialization process, design transfer to manufacturing process, and marketing and sales. Specifically, the phantom box will be injection molded to increase the box's durability by making it airtight and preventing leaks during the curing process. Supplemental Figure 4 shows the first iteration of a 3D printed version of the silicone backfilling mold, another step of the continuation of the commercialization process. Eventually, 3D printing will be contracted out to an outside vendor to increase print reliability and speed of production. The commercialization process will occur between

April and July of 2020. The design transfer to manufacturing will occur in August 2020. Staff training will be incorporated into the design transfer. Then, the marketing and sales will begin in September 2020. Sales will target academic training centers and meet international distributor needs by providing training tools for sales representatives.

Ultimately, the developed lumbar spinal phantom has a self-healing shown within 24 hours, an attenuation similar to an ATS phantom, negligible insertion loss, a transparent color, an acceptable tack level, a lifetime of greater than 10 years, and a speed of sound statistically equivalent to human tissue. Given these characteristics and its ability to deliver superior performance during training when compared to any other commercial phantom, the developed lumbar spinal phantom can be characterized as novel and innovative for its field.

Materials & Methods

Tissue and Skin Layer Recipes and Layer Combination

The finalization of the tissue and skin components of the spinal phantom was completed using a mixture of a two-part polyurethane (RM16 A/B), a filler (terphenyl), and an ultrasound scatterer. Additionally, gloves and a scale were required. To finalize the skin and tissue layer recipe, the RM16 A:B ratio was manipulated.

First, the tissue layer recipe was finalized. This finalization was based on iterative RM16 A:B ratio testing which proceeded according to Table 1 in the results section. Once the tissue layer was finalized, a container was placed on the scale and the scale was zeroed. The required liquid RM16A mass was dispensed into the container. The liquid was allowed to settle into the bottom of the container before proceeding. Then, the desired scatterer mass was added to the mix. The liquid was mixed with a tongue depressor. This process was repeated with the desired terphenyl mass. Next, the scale was zeroed and the required liquid RM16B mass was dispensed into the container. Mixing with the tongue depressor began immediately and focused on mixing in the corners and troughs of the container to create homogeneity. To remove the air from the mixture, the container was placed in a vacuum chamber. The vacuum was turned on until the pressure approached -29 mmHG on the gauge. The mixture was observed for the foaming and subsequent cratering of the mixture. Once the mixture cratered, it was removed from the vacuum chamber. Next, the mixture was placed in an oven. To finalize the skin layer recipe, the tissue layer procedure should be repeated with the desired A:B ratio iteratively obtained according to the criteria in Table 1, displayed above.

Upon the finalization of the skin and tissue layer recipes, the skin and tissue layer were combined to create the spinal phantom. To allow for the multiple layers, the tissue layer was cured first until a jelly-like consistency was obtained. Next, the skin layer was added. To prevent marring of the tissue layer, the container was tilted to the side when mixing the skin layer components. Next, the container was vacuumed to remove air from the mixture. The container then cured with the tissue and skin layer combined to create the spinal phantom. To prevent material waste, the RM16A and RM16B squeeze bottles were purged with Argon gas for 15 seconds each.

Self-Healing Testing

First, the tissue layer was "injured." This was done by injecting and removing an epidural needle from the tissue layer, leaving a needle track. The epidural needle, a longer needle with a curve on the end, was used to exaggerate the injuries of the phantom. In the final version of the phantom, a practice needle will be included that does not have a curve and will not be as likely to injure the phantom. Second, a time-lapse video camera was used to record the self-healing progression of the spinal phantom. The camera collected images at a 15 second interval while recording for 24 hours.

Acoustic Characterization

After the finalization of the skin and tissue layers, the acoustic characterization was conducted. This testing involved the materials' speed of sound, acoustic attenuation, and injection loss. The acoustic characterization data was obtained by Acertara Acoustic Laboratories, an ISO accredited test facility which agreed to test the skin and tissue layers as well as other potential formulations.[13] The test facility also provided performance data of the Rivanna tissue layer with respect to surface tack, color, and phantom lifetime.

Backfilling the Spinal Canal and Silicone Mold Development

To be able to make the phantom spine more similar to the *in vivo* human spine, the spinal canal was filled with polyurethane that does not contain the scatterer contained in the tissue and skin mixtures. This was done because *in vivo* the area within the spine does not scatter ultrasound signals like human tissue does. This results in that area showing up dark on an ultrasound readout. To emulate this, the spinal canal had to be backfilled with polyurethane that did not contain scatterers. Backfilling, or inverting and filling the canal from the bottom, was required because the gaps in the posterior of the spine would leak polyurethane if filled from the anterior.

A silicone negative of the spine was cast. This blue silicone negative can be seen below the 3D printed spine in Figure 4, as well as in Supplemental Figure 5. This negative cast supports the backfilling of the spine because it covered the gaps in the posterior of the spine. The cast also allowed the spinal canal polyurethane to fill the gaps only up to the exterior of the spine. To prevent leakage of the spinal canal polyurethane, once the spine was inverted and placed on the silicone mold, the spine was adhered to the mold using masking silicone. Any gaps in the spine, such as the foramen, were also closed with masking silicone. Once the masking silicone was applied, the backfilling apparatus, as seen in Supplemental Figure 4, was left at room temperature for 24 hours to allow for the masking silicone to cure. The backfilling itself was conducted through three holes in the anterior of the 3D printed spine. The polyurethane was mixed in a cup then drawn up into a syringe. A needle attachment was added to the syringe and the polyurethane was injected into the hole closest to the bottom of the spine, as seen in Figure 4. Additionally, the apparatus was placed at a slight incline with the injection hole at the bottom in order to push air up the spinal canal and prevent bubble formation inside the canal. Once the polyurethane was in excess in the canal such that adding additional material pushed polyurethane out of the injection holes, the apparatus was placed in the vacuum. After 3 minutes, the apparatus was removed and left on an incline at room temperature for 1 hour to allow more air to escape. After 1 hour, the apparatus was placed in an oven at 65 °C overnight. The next day, the apparatus was removed from the oven and the spine was peeled off of the silicone mold. The final backfilled spine can be seen in Supplemental Figure 6 below. As shown in the figure, the polyurethane is contoured to the gaps of the spinal canal so that only the canal will lack scatterers.

Figure 4: This figure displays the spinal backfilling process. Backfilling of the spinal column is performed to make the phantom realistic and provide consistent results when scanned with the Accuro. *Backfilling consisted of inverting the 3-D printed spine onto a silicone mold cast of the top of the spine. The spine was then adhered to the silicone mold using a masking silicone adhesive. Then, a specialized mixture of polyurethane without scatterers was injected through the holes on the bottom of the spine, as shown in this figure.*

Curing Method Finalization

The curing method finalization involved the manipulation of time and heat exposure involved in the curing process in order to minimize settling of the scatterers, which are micron-dimensioned solid particles. Ultrasound imaging was performed at 7.5 MHz with Alpinion Linear Array (fundamental-mode imaging) to observe the settling. These images are shown above in Figure 3. The curing process associated with the image was evaluated based on the level of scatterer distribution shown.

The curing method was finalized as follows. First, the required mass of RM16A was dispensed into a container. Then, the scatterer and terphenyl masses were added and thoroughly mixed into the container. Then, the required mass of RM16B was

dispensed into a separate container. Once the mixture of RM16A, terphenyl, and the scatterer was mixed with RM16B, a 50-minute timer was started. The combined mixture was mixed using a paint stirrer to ensure that polyurethane on the sides and bottom of the container was well mixed. The mixture was also poured back and forth between the buckets that contained RM16A and RM16B to further ensure the mixture's homogeneity. This was done for 2 minutes, then the mixture was vacuumed to remove the air introduced by the mixing process. After vacuuming for about 5 minutes, the mixture sat out for the remainder of the 50 minutes to continue to remove air before curing. At 40 minutes, the phantom box containing the 3D printed spine and stand adhered to the bottom was placed in the oven set to 110℃ to preheat. At 50 minutes, the mixture was lightly mixed with a paint stirrer while trying to introduce as little air as possible into the mixture. This was done for 2 minutes. Then, the phantom box was removed from the oven and the mixture was poured in at an angle to reduce the air being introduced in the mixture. Once the mixture was in the phantom box, the stirrer was used to stir the sides and the top of the phantom lightly. Then, the box was vacuumed to further reduce the air in the mixture. This was done for about 5 minutes. Once completed, the box was placed in the oven at 110℃ for 30 minutes. If the mixture was not appropriately viscous after 30 minutes, additional time was added in 10-minute increments to ensure adequate curing. This process was the same for the skin and tissue layers.

Productization

To initiate the productization timeline, Rivanna Medical's requirements for the product were identified. First, the phantom's dimensions were identified. These dimensions dictated that the phantom had to have dimensions of at least 15cm depth, 12.7cm width, and 12.7cm length. Additionally, Rivanna required the phantom box include a lid and have transparent walls. A temporary box that satisfied these requirements was purchased. This prototype box was used for the development of the spinal phantom. The prototype box was a plexiglass cube with one open side and a lid. Figure 5 displays a 3-D printed spine with a backfilled spinal canal that is adhered to a stand inside of a prototype box, demonstrating what the box looks like prior to pouring the skin and tissue layers. These boxes were found to not be airtight, so masking silicone was used to seal the edges of the box.

Research was conducted on the existing spinal phantom that Rivanna purchases as well as alternative phantoms to identify potential features to include. From these existing commercial phantoms, a handle and brand label were identified as features that could be applied to Rivanna's phantom. Upon identification, Rivanna agreed to the inclusion of these features and a needle holster. This feature, not currently offered by other commercial phantoms, would allow doctors to safely store the practice needle on the side of the phantom. This holster must be long enough to contain the entire practice needle safely while still allowing its withdrawal. The practice needle is a specialized tool that prevents the needle from creating unnecessary gashes or injuries to the phantom.

Figure 5: This figure shows a 3-D printed spine with a backfilled spinal canal adhered to a stand inside the prototype box. *This demonstrates what the box looked like prior to pouring the skin and tissue layers.*

Creation of 3 full phantoms

Once consistent backfilling was achieved, the goal was to successfully create three full-scale phantoms. These consisted of the skin and tissue layers, backfilled, 3D printed spine, and stand. The full-scale phantom was created by pouring the required materials, vacuuming, and curing overnight. Each full-scale phantom contained the 3D printed spine, a 3D printed stand, the tissue layer, and the skin layer in the prototype box. The spine was held in place by a 3D printed, translucent

stand. This stand was nearly invisible when viewed through the tissue layer. Figure 6 shows a full-scale phantom. In the figure, it can be seen that both the skin and tissue layers of the phantom are translucent.

Figure 6: This figure shows a full-scale phantom in a prototype box. *The full-scale phantom contains the spine, a stand, the tissue layer, and the skin layer in a prototype box with a lid. Both layers of the phantom are translucent. The 3D printed spine is held in place by a 3D printed, translucent stand, which is difficult to observe from this angle. The prototype box is a plexiglass cube with one open side and a lid. This box will not be used in manufacture of the product because it is not airtight and leaks during the curing process.*

End Matter

Author Contributions and Notes

V.P., J.M., and A.D. designed research, V.P., J.M., A.D., and R.N. performed research, V.P. and J.M. analyzed data; and V.P. and J.M. wrote the paper. The authors declare no conflict of interest

Acknowledgments

We would like to thank Adam Dixon, our advisor at Rivanna Medical, for providing help and advice constantly on the project. We would also like to thank Rachel Newman of Rivanna Medical, who helped advance the project in the Spring Semester. Furthermore, we would like to thank all the staff of Rivanna Medical for making the project an education and enjoyable experience. Finally, we would like to thank Acertara Acoustic labs for running the acoustic characterization tests.

References

1. Park DK. Spinal injections. OrthoInfo. https://www.orthoinfo.org/en/treatment/spinal-injections/. Published August 2018. Accessed October 20, 2019.
2. Arendt K, Segal S. Why epidurals do not always work. *Rev Obstet Gynecol*. 2008;1(2):49-55.
3. Clinical value. https://rivannamedical.com/clinical-value/. Accessed October 20, 2019.
4. Materese R. What are imaging phantoms? NIST. https://www.nist.gov/topics/physics/what-are-imaging-phantoms. Published April 19, 2018. Accessed October 21, 2019.
5. Dixon A. E-mail correspondence between Capstone Advisor Adam Dixon and the Capstone Team. August 2019.
6. Woodford C. How do self-healing materials work? Explain that Stuff. http://www.explainthatstuff.com/self-healing-materials.html. Published March 23, 2019. Accessed October 29, 2019.
7. Lumbar-Spine Training Phantom. https://rivannamedical.com/wp-content/uploads/2016/10/Accuro-Training-Phantom.pdf.
8. Ultrasound FAQ. CIRS. https://www.cirsinc.com/support/faq/. Accessed April 21, 2020.
9. Multi-Purpose Phantom: Model ATS 539. 2013. http://www.cirsinc.com/wp-content/uploads/2020/03/ATS-539-DS-032420.pdf. Accessed April 21, 2020.
10. Overview for 1-Sample Equivalence Test. https://support.minitab.com/en-us/minitab/18/help-and-how-to/statistics/equivalence-tests/how-to/1-sample-equivalence-test/before-you-start/overview/. Accessed April 22, 2020.
11. Stern B. The Basic Concepts of Diagnostic Ultrasound1. Yale-New Haven Teachers Institute. https://teachersinstitute.yale.edu/curriculum/units/1983/7/83.07.05.x.html. Published 1983. Accessed April 22, 2020.
12. Wilson M, Coleman M, McGrath J. Developing basic hand-eye coordination skills for laparoscopic surgery using gaze training. *BJU Int*. 2010;105(10):1356-1358. doi:10.1111/j.1464-410X.2010.09315.x
13. Acertara: Diagnostic Ultrasound Probes, Equipment & Service. Acertara. https://www.acertaralabs.com/. Accessed April 21, 20

Supplemental Material

Supplemental Figure 1: The image depicts the current commercial spinal phantom that Rivanna Medical packages with Accuro. *The current phantom has limitations. These limitations are described in the Introduction section.*

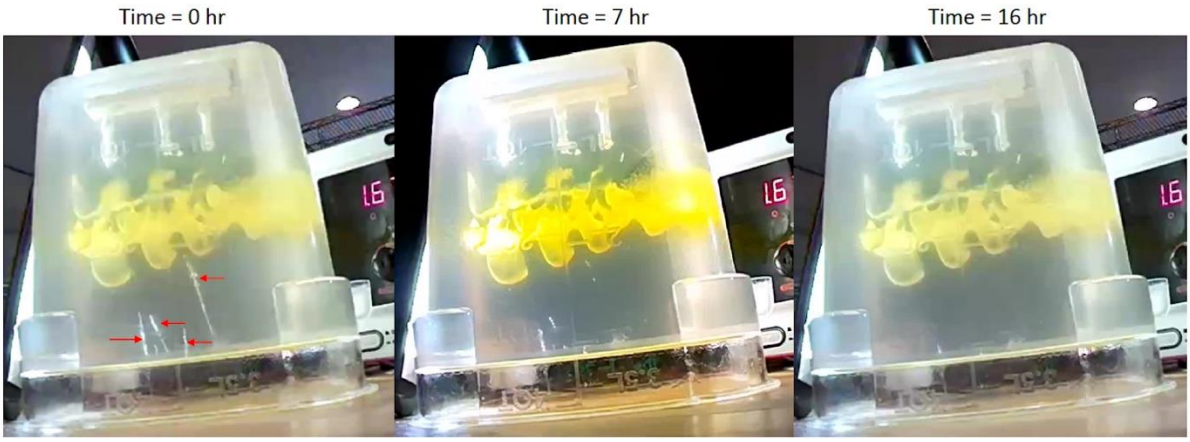

Supplemental Figure 2: The figure shows the self-healing progression of the spinal phantom. *First the tissue layer was "injured." This was done by injecting and removing an epidural needle from the tissue layer. This left a needle track. The red arrows point to the needle tracks. Second, a timelapse video camera was used to record the self-healing progression. This image displays images of the self-healing at specific time points: 0 hours, 7 hours, and 16 hours.*

WORKSHEET 1

One-Sample Equivalence Test: Tissue Layer

Method

Target = 1540
Lower equivalence limit = -0.05 × target = -77
Upper equivalence limit = 0.05 × target = 77

Descriptive Statistics

Variable	N	Mean	StDev	SE Mean
Tissue Layer	3	1527.5	3.2967	1.9034

Difference: Mean(Tissue Layer) - Target

Difference	SE	99.9% CI for Equivalence	Equivalence Interval
-12.503	1.9034	(-55.0001, 29.9934)	(-77, 77)

CI is within the equivalence interval. Can claim equivalence.

Test

Null hypothesis: Difference ≤ -77 or Difference ≥ 77
Alternative hypothesis: -77 < Difference < 77
α level: 0.001

Null Hypothesis	DF	T-Value	P-Value
Difference ≤ -77	2	33.886	0.0004349
Difference ≥ 77	2	-47.024	0.0002260

The greater of the two P-Values is 0.000. Can claim equivalence.

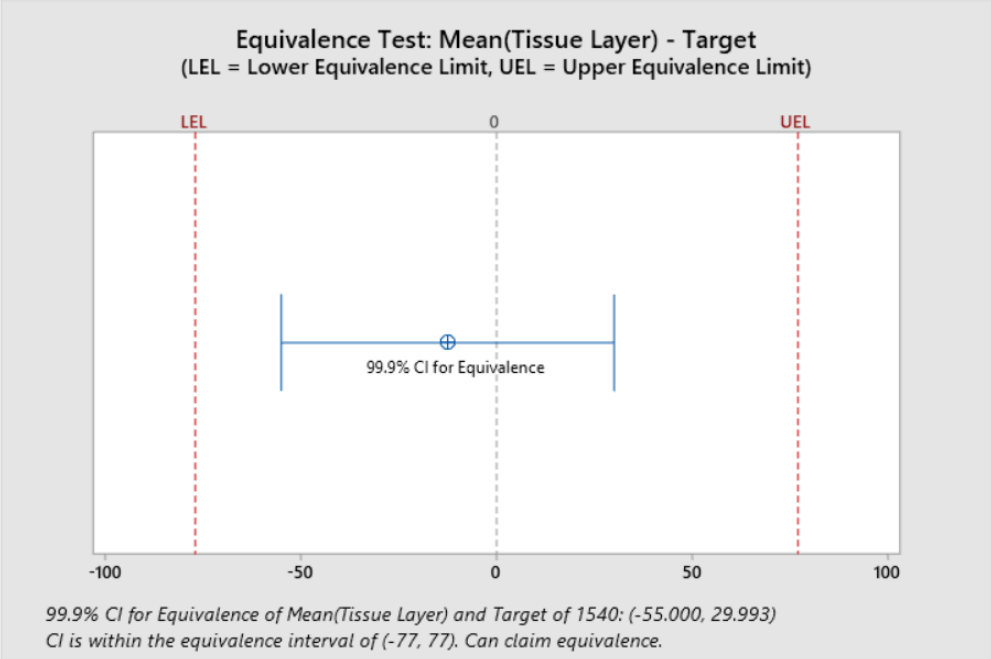

Supplemental Figure 3: This figure displays the one-sample equivalence test for the tissue layer. *The method, descriptive statistics, difference, and test information is included in this figure. Additionally, the equivalence testing graph is displayed.*

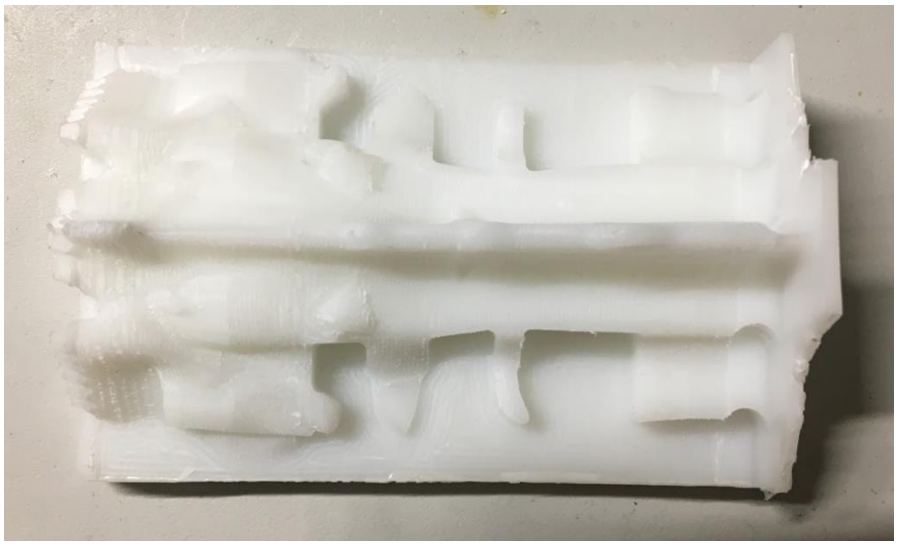

Supplemental Figure 4: The figure shows the continuation of the commercialization phase. *The silicone mold will be replaced by a 3D printed part. Eventually, the 3D printing process will be contracted to an outside vendor to increase reliability and speed of production.*

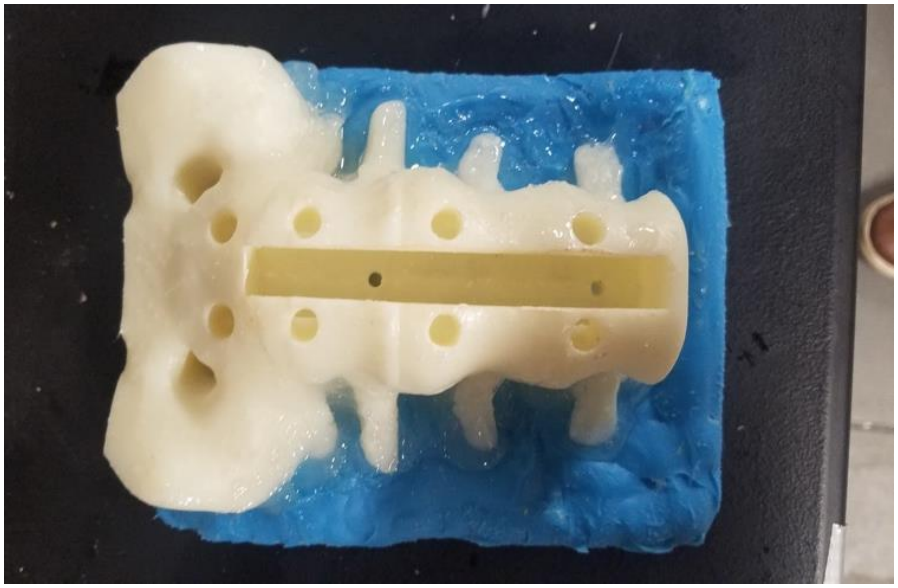

Supplemental Figure 5: The figure depicts the spinal backfilling apparatus. *A silicone negative of the spine was cast to support the backfilling of the spine. Once the spine was inverted and placed on the silicone mold, it was adhered using masking silicone to prevent leakage.*

Supplemental Figure 6: The image depicts the backfilled spinal canal. *The spinal canal was backfilled with polyurethane. This was done to make the phantom spine more similar to the in vivo human spine.*

Supplemental Table 1: The table shows the results of the average pixel intensity, standard deviation of pixel diversity, and the coefficient of variation for two scatterer distributions. *These calculations were performed to demonstrate the differences between an area with heterogeneous scatterer distribution and an area with homogeneous scatterer distribution.*

Scatterer Distribution	Average Pixel Intensity	Standard Deviation of Pixel Density	Coefficient of Variation
Homogeneous	114.87	20.29	0.177
Heterogeneous	59.66	32.32	0.542